CrossMark

Quantitative sonographic image analysis for hepatic nodules: a pilot study

Naoki Matsumoto[1] · Masahiro Ogawa[1] · Kentaro Takayasu[1] · Midori Hirayama[1] ·
Takao Miura[1] · Katsuhiko Shiozawa[1] · Masahisa Abe[1] · Hiroshi Nakagawara[1] ·
Mitsuhiko Moriyama[1] · Seiichi Udagawa[2]

Abstract

Purpose The aim of this study was to investigate the feasibility of quantitative image analysis to differentiate hepatic nodules on gray-scale sonographic images.

Methods We retrospectively evaluated 35 nodules from 31 patients with hepatocellular carcinoma (HCC), 60 nodules from 58 patients with liver hemangioma, and 22 nodules from 22 patients with liver metastasis. Gray-scale sonographic images were evaluated with subjective judgment and image analysis using ImageJ software. Reviewers classified the shape of nodules as irregular or round, and the surface of nodules as rough or smooth.

Results Circularity values were lower in the irregular group than in the round group (median 0.823, 0.892; range 0.641–0.915, 0.784–0.932, respectively; $P = 3.21 \times 10^{-10}$). Solidity values were lower in the rough group than in the smooth group (median 0.957, 0.968; range 0.894–0.986, 0.933–0.988, respectively; $P = 1.53 \times 10^{-4}$). The HCC group had higher circularity and solidity values than the hemangioma group. The HCC and liver metastasis groups had lower median, mean, modal, and minimum gray values than the hemangioma group. Multivariate analysis showed circularity [standardized odds ratio (OR), 2.077; 95 % confidential interval (CI) = 1.295–3.331; $P = 0.002$] and minimum gray value (OR 0.482; 95 % CI = 0.956–0.990; $P = 0.001$) as

factors predictive of malignancy. The combination of subjective judgment and image analysis provided 58.3 % sensitivity and 89.5 % specificity with AUC = 0.739, representing an improvement over subjective judgment alone (68.4 % sensitivity, 75.0 % specificity, AUC = 0.701) ($P = 0.008$).

Conclusion Quantitative image analysis for ultrasonic images of hepatic nodules may correlate with subjective judgment in predicting malignancy.

Keywords Quantitative image analysis · Ultrasonography · Hepatocellular carcinoma · Liver hemangioma · Liver metastasis

Introduction

Imaging evaluation of hepatic nodules is usually based on the subjective judgment of the sonographer or radiologist. Diagnostic accuracy can thus vary with experience. Quantitative image analysis might be helpful to improve imaging diagnosis even for readers with less experience.

Ultrasound image analysis for the diagnosis of liver disease has been performed based on: texture analysis for chronic liver disease [1–6]; diagnosis of hepatic tumors using a time–intensity curve during contrast-enhanced ultrasonography [7]; and assessment of liver fibrosis according to the arrival time of the contrast agent [8].

Morphological ultrasound image analysis of hepatic tumors has been performed with artificial neural networks [3, 9, 10] and computer-aided algorithms [11]. In those reports, image analysis was used for classification into hepatocellular carcinoma (HCC), liver metastasis, hemangioma, or cyst. In addition, software for image analysis has recently become easily accessible on the internet for free [12].

✉ Naoki Matsumoto
matsumotosg7@gmail.com

1   Division of Gastroenterology and Hepatology, Department of Medicine, Nihon University School of Medicine, 30-1 Oyaguchi Kamimachi, Itabashi, Tokyo 173-8610, Japan

2   Department of Mathematics, Nihon University School of Medicine, 30-1 Oyaguchi Kamimachi, Itabashi, Tokyo 173-8610, Japan

🄐 Springer

The present study applied this technique for the evaluation of hepatic nodules. The aim of this study was to investigate the feasibility of quantitative image analysis to differentiate hepatic nodules.

Materials and methods

Patients

Patients were randomly selected from among those with hepatic nodules who underwent ultrasonography between January 2004 and July 2014. The study group comprised 71 men and 40 women (median age 67 years; range 17–91 years). Median tumor size was 23 mm (range 6–67 mm). We retrospectively evaluated 35 nodules from 31 patients with histopathological evidence of HCC (1 early HCC, 4 well-differentiated HCCs, 23 moderately differentiated HCCs, and 7 poorly differentiated HCCs), 60 nodules from 58 patients with liver hemangioma, and 22 nodules from 22 patients with liver metastases that had been previously confirmed on contrast-enhanced ultrasonography, contrast-enhanced computed tomography, or contrast-enhanced magnetic resonance imaging (Table 1).

This cross-sectional study was performed in accordance with the principles of the Declaration of Helsinki. Comprehensive informed consent regarding the use of data was obtained in writing from each subject. Clinical data including serological and follow-up data were obtained from hospital records for all cases. The institutional review board of our university judged that this retrospective study did not require board approval.

Imaging techniques

LOGIQ 7 or LOGIQ E9 ultrasonic equipment (GE Healthcare Japan, Tokyo, Japan) was used in this study with a 9L linear transducer (frequency, 9 MHz). Sonographic examination was performed with the patient in the decubitus position under fasting conditions. The right arm of the patient was elevated and respiratory conditions were modified properly. A sonographic image was captured at maximum diameter of the tumor by an experienced operator. Dynamic range and gain were not altered. A single focus was set at the deepest margin of the nodule. Tissue harmonic imaging was used in all cases. The acquired data were digitally stored on a hard disk as raw data.

Imaging analysis

Image data captured at maximum tumor diameter were saved in JPEG format on a personal computer and analyzed using ImageJ version 1.47 software (National Institutes of Health, available at http://rsb.info.nih.gov/ij). Outlines of hepatic nodules were drawn free-hand by three hepatologists who were board-certified Fellows of the Japan Society of Ultrasonics in Medicine (FJSUM), and analyzed in "ROI Manager" mode. Analyzed values were circularity, solidity, aspect ratio, median gray value, mean gray value, modal gray value, minimum gray value, maximum gray value, and standard deviation of gray value. These parameters were automatically calculated using ImageJ software. Each analyzed value was defined as follows (Figs. 1, 2) [12].

$$\text{Circularity} = 4\pi \times \frac{[\text{Area}]}{[\text{Perimeter}]^2}$$

$$\text{Solidity} = \frac{[\text{Area}]}{[\text{Convex} \cdot \text{area}]}$$

$$\text{Aspect ratio} = \frac{1}{4} \times \frac{\pi \times [\text{Major} \cdot \text{axis}]^2}{[\text{Area}]}$$

Median gray value = median gray-scale value within the selected region of interest. This is the sum of the gray values of all pixels in the selection divided by the number of pixels.

Mean gray value = average gray-scale value within the selected region of interest.

Modal gray value = most frequently occurring gray value within the selected region of interest.

Table 1 Patient characteristics

	HCC	Liver metastasis	Hemangioma	*P*
n	35 (31 cases)	22	60 (58 cases)	
Age	72 (41–85)	68 (51–91)	58 (35–82)	<0.001
Male/female	18/13	17/5	36/22	0.486
NL/FL/CH/LC	0/0/16/21	22/0/0/0	37/7/7/7	1
Size (mm)	25 (6–55)	23.5 (11–50)	16 (9–67)	0.795
Location (right lobe/left lobe)	26/8	15/7	44/14	0.874

A significant difference was observed in age among the three groups

One case of HCC arose at the caudate lobe

HCC hepatocellular carcinoma, *NL* normal liver, *FL* fatty liver, *CH* chronic hepatitis, *LC* liver cirrhosis
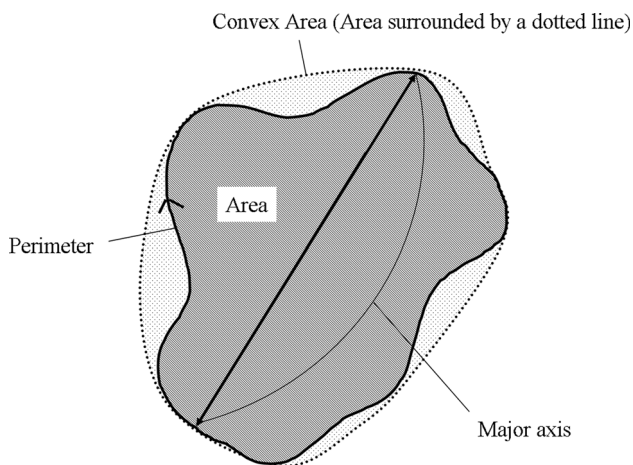
Fig. 1 Illustration for circularity, solidity, and aspect ratio. These parameters are calculated from area (area surrounded by a *solid line*), convex area (area surrounded by a *dotted line*), perimeter, and major axis. Convex area can be thought of as a rubber band wrapped tightly around the area

Minimum and maximum gray value = minimum and maximum gray-scale values within the selected region of interest.
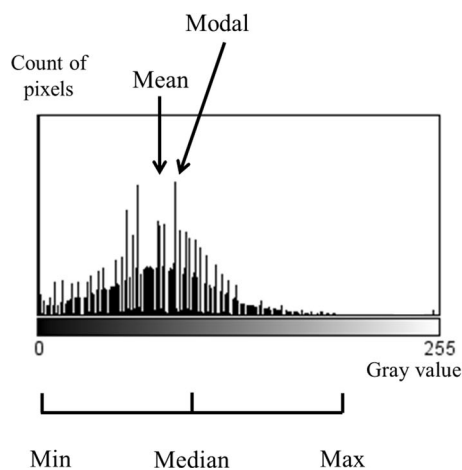
Standard deviation = standard deviation of gray-scale values used to generate the mean gray-scale value.

The range of gray values between Min and Max is divided into 256 bins.

Validation study

Three hepatologists drew outlines of the same image of HCC, metastasis, and hemangioma, with each making 10 attempts. Data obtained from ROI Manager were analyzed. Each value was validated using the Smirnov–Grubbs test.

Subjective judgment of ultrasonic images

All images were reviewed independently by three readers who had experience in abdominal ultrasonography. When two or three reviewers provided the same opinion, that opinion was accepted as the result. If all three reviewers offered different opinions, the case was excluded from analysis. The readers had no knowledge of the results of other imaging modalities or the histological diagnosis.

All hepatic nodules were classified by echogenicity into "hyper," "iso," "hypo," or "mixed" patterns, by shape into "irregular" or "round," and by surface into "rough" or "smooth." Halo, mosaic pattern, and lateral shadows were recognized as features of malignancy [13].

Statistical analysis

Data are expressed as mean ± standard deviation. The statistical significance of sonographic image findings was calculated using the Mann–Whitney U test and the Chi-square test. Kruskal–Wallis test was used in Tables 1, 2, and 3 for comparison between each group. Multivariate analysis was carried out by logistic regression with the backward elimination method. Values of $P < 0.05$ were considered statistically significant for all analyses. The Statistical Program for Social Sciences software package (SPSS 11.5 for Windows, SPSS, Chicago, IL) was used to perform statistical analysis.

Results

Validation of reproducibility for drawing outlines of each hepatic tumor

Outliers were detected for standard deviation of HCC, median gray value and solidity of liver metastasis, and
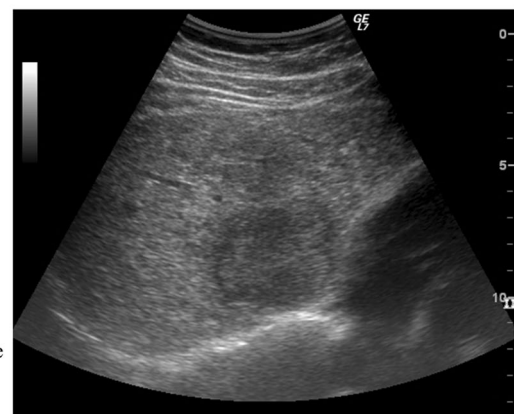
Fig. 2 Illustration for median, mean, modal, minimum, and maximum gray values. Histogram (*left*) revealed the gray value of the hepatic tumor (*right*)

Table 2 Comparison between subjective judgement and image analysis

	Hyperechoic	Isoechoic	Hypoechoic	Mix pattern	P
n	66	4	28	19	
Median gray value	80 (29–153)	77 (48–119)	63 (17–113)	66 (39–122)	0.097
Mean gray value	80.6 (30.4–151.4)	76.6 (49.9–118.9)	66.1 (19.3–115.1)	68.2 (40.2–124.1)	0.142
Modal gray value	80 (0–159)	71.5 (41–113)	60.5 (10–119)	68 (36–121)	0.131
Minimum gray value	31.5 (0–104)	35.5 (0–79)	25 (0–79)	20 (0–73)	0.562
Maximum gray value	148.5 (80–237)	137.5 (115–168)	128.5 (68–214)	144 (103–219)	0.208
Standard deviation	17.8 (11.9–41.4)	15.5 (14.0–18.7)	14.2 (8.8–30.0)	18.9 (12.6–29.5)	0.001

Standard deviation was higher in the hyperechoic group than in the hypoechoic group

Table 3 Image analysis of each hepatic nodule

	HCC	Liver metastasis	Hemangioma	P		
				HCC vs. metastasis	HCC vs. hemangioma	metastasis vs. hemangioma
Circularity	0.892 (0.776–0.927)	0.882 (0.651–0.932)	0.848 (0.641–0.928)	N.S.	<0.001	0.038
Solidity	0.972 (0.932–0.983)	0.791 (1.491–0.976)	0.956 (0.894–0.986)	N.S.	<0.001	0.002
Aspect ratio	1.240 (1.014–1.954)	1.264 (1.025–2.037)	1.280 (1.040–2.524)	N.S.	N.S.	N.S.
Median gray value	65 (21–137)	54 (17–119)	81.5 (29–153)	N.S.	0.005	0.005
Mean gray value	66.8 (22.1–135.6)	54.4 (19.3–118.9)	82.4 (30.4–151.4)	N.S.	0.005	0.005
Modal gray value	60.0 (21–129)	51.0 (0–113)	80.0 (0–159)	N.S.	0.007	0.007
Minimum gray value	17.0 (0–73)	10.5 (0–79)	38.5 (0–104)	N.S.	0.002	0.025
Maximum gray value	145.0 (68–214)	123.0 (71–202)	150.5 (93–237)	N.S.	N.S.	N.S.
Standard deviation	18.6 (10.1–30.0)	15.9 (8.8–41.4)	17.0 (10.5–29.5)	N.S.	N.S.	N.S.

HCC hepatocellular carcinoma

median gray value of hemangioma. Other data were not detected as outliers (Fig. 3). Mean values for HCC were as follows: aspect ratio 1.237 (range 1.161–1.297); circularity 0.895 (range 0.823–0.939); solidity 0.975 (range 0.954–0.982); minimum gray value 18 (range 18–21); maximum gray value 144 (range 144–144); median gray value 65 (range 63–66); mean gray value 66.3 (range 65.2–67.5); modal gray value 60 (range 60–71); and standard deviation of gray value 22.8 (range 22.3–23.0).

Mean values for hemangioma were as follows: aspect ratio 1.203 (range 1.143–1.266); circularity 0.820 (0.754–0.875); solidity 0.960 (0.926–0.977); minimum gray value 14 (12–14); maximum gray value 173 (153–207); median gray value 68 (67–70); mean gray value 69.1 (67.8–70.4); modal gray value 71 (71–71); and standard deviation of gray value 20.9 (18.4–21.2).

Mean values for liver metastasis were as follows: aspect ratio 1.849 (range 1.667–1.992); circularity 0.745 (0.680–0.784); solidity 0.947 (0.920–0.963); minimum gray value 5 (5–6); maximum gray value 130 (111–156); median gray value 47 (43–49); mean gray value 49.2 (45.4–51.6); modal gray value 43 (43–43); and standard deviation of gray value 19.8 (17.0–21.6).

## Comparison of subjective judgment and image analysis

Hepatic nodules were judged as hyperechoic ($n = 60$), isoechoic ($n = 4$), hypoechoic ($n = 28$), or mixed pattern ($n = 19$) by the three reviewers (Table 2). Median, mean, modal, minimum, and maximum gray values showed no significant differences among the four echogenicity groups. Standard deviation was higher in the hyperechoic group than in the hypoechoic group ($P = 0.001$).

Circularity was lower in the irregular group (median 0.823, range 0.641–0.915) than in the round group (median 0.892, range 0.784–0.932, $P = 3.21 \times 10^{-10}$). Solidity was lower in the rough group (median 0.957, range 0.894–0.986) than in the smooth group (median 0.968, range 0.933–0.988, $P = 1.53 \times 10^{-4}$) (Fig. 4).

Image analysis findings for each tumor

HCC and liver metastasis showed higher circularity and solidity than hemangioma (Table 3). HCC and liver metastasis displayed lower median, mean, modal, and minimum gray values than hemangioma. Aspect ratio and standard deviation showed no significant differences.

Fig. 3 Validation of reproducibility for drawing outline of HCC, metastasis, and hemangioma with longitudinal axis as value of data. *AR* aspect ratio, *Min* minimum gray value, *Max* maximum gray value, *Median* median gray value, *Mean* mean gray value, *Mode* modal gray value, *StdDev* standard deviation
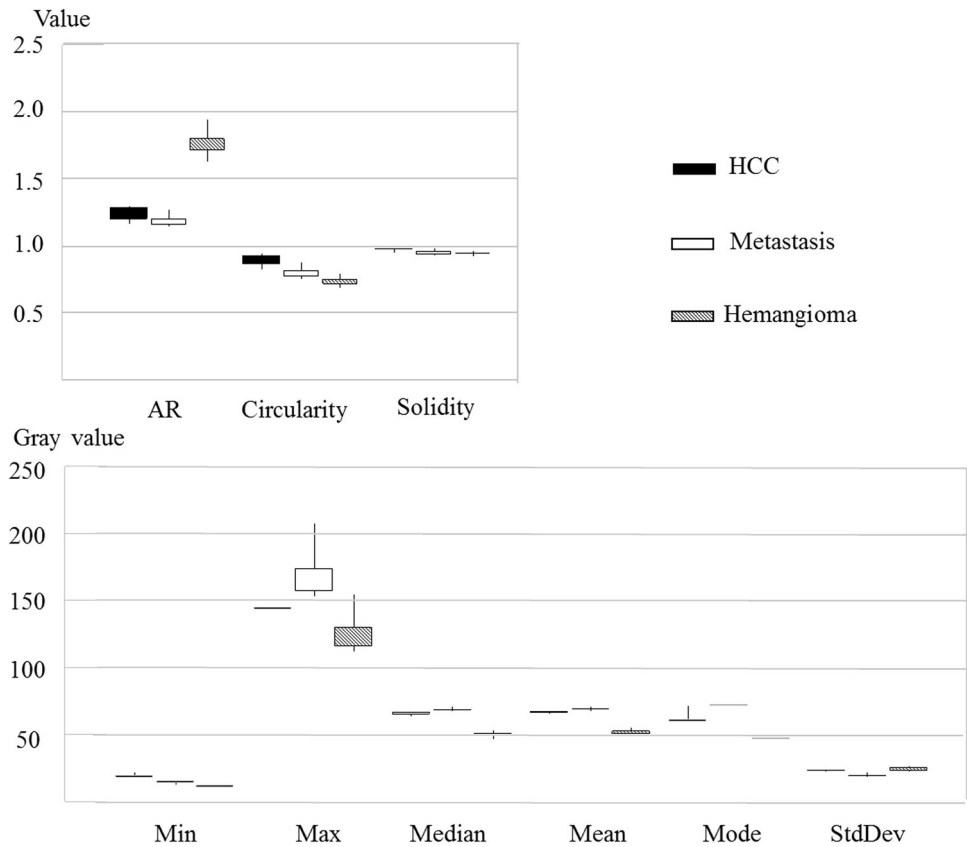
Multivariate analysis of malignancy on image analysis

Univariate findings revealed significant differences in circularity, solidity, median, mean, modal, and minimum gray values. Multivariate analysis showed circularity [standardized odds ratio (OR), 2.077; 95 % confidential interval (CI) = 1.295–3.331; $P = 0.002$] and minimum gray value (OR 0.482, 95 % CI = 0.956–0.990, $P = 0.001$) as factors predictive of malignancy (Table 4).

Diagnostic accuracy of combining subjective judgment and image analysis

The prevalence of halo, mosaic pattern, and lateral shadows in the malignancy (HCC and metastasis) group and hemangioma group was 47.4 % vs. 6.8 % ($P = 5.88 \times 10^{-7}$), 24.6 % vs. 3.4 % ($P = 9.73 \times 10^{-4}$), and 31.6 % vs. 3.4 % ($P = 4.64 \times 10^{-5}$), respectively.

When two of the predictive factors based on subjective judgment (halo, mosaic pattern, or lateral shadow) were positive, the area under the curve (AUC) for malignancy was 0.623 (sensitivity 26.3 %; specificity 98.3 %).

Regarding imaging analysis, circularity offered 54.4 % sensitivity, 78.3 % specificity, and 0.888 cutoff with

AUC = 0.704. Minimum gray value offered 68.4 % sensitivity, 75.0 % specificity, and 22.0 cutoff with AUC = 0.701.

The combination of subjective judgment and image analysis provided 58.3 % sensitivity and 89.5 % specificity with AUC = 0.739, representing an improvement over subjective judgment alone ($P = 0.008$) (Fig. 5).

Discussion

In this study, image analysis correlated with subjective judgment in terms of shape and surface, but echogenicity revealed some discordance. The diagnostic accuracy of malignancy was improved by adding image analysis to subjective judgment. Image analysis showed differences among HCC, liver metastasis, and hepatic hemangioma. HCC and metastasis showed higher circularity and solidity values and lower median, mean, modal, and minimum gray values compared to hemangioma. In other words, HCC and metastasis showed smoother outlines and more circular shapes, and were more hypoechoic compared to hemangioma.

Sonographic gray-scale findings of hepatic tumor have been described in various reports [13–15]. Although color Doppler imaging and contrast-enhanced ultrasonography
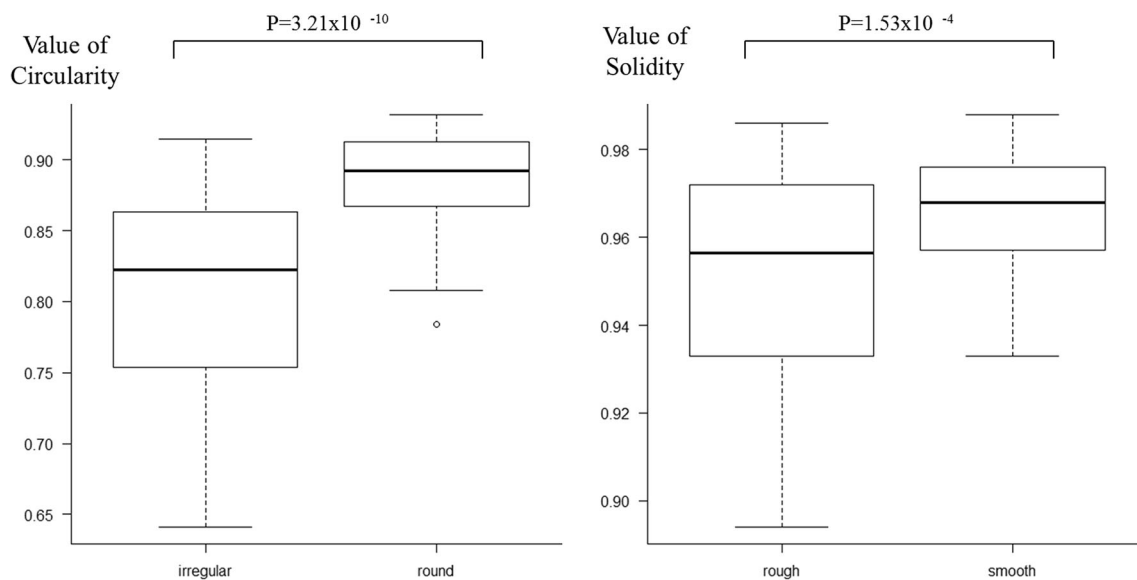
Fig. 4 Circularity was lower in the irregular group than in the round group (*left*), and solidity was lower in the rough group than in the smooth group (*right*)

Table 4 Multivariate logistic regression for diagnosis of malignancy

	Unstandardized regression coefficients	Standardized regression coefficients	Standard error	95 % confidential interval	OR	*P*
Circularity	10.837	0.731	0.241	1.295–3.331	2.077	0.002
Minimum gray value	−0.032	−0.731	0.225	0.310–0.749	0.482	0.001

All variables ware standardized. Odds ratios were expressed per standardized unit

provide large amounts of information, gray-scale findings remain important to diagnose hepatic tumors. HCCs typically show features of a hypoechoic rim, mosaic pattern, posterior echo enhancement, and lateral shadows [13]. Hepatic hemangiomas have an irregular shape, clear borders, and hyperechoic rim [13, 15]. Previous reports have described 77.1 % of hemangiomas as hyperechoic [15]. Liver metastasis occasionally shows a thick hypoechoic rim appearing as a "bull's eye" [16]. Morphological features of hepatic tumors have been decided based on the subjective opinions of operators rather than quantitative analysis to date. In the present study, image analysis revealed the form and color of each type of tumor.

Ultrasound image analysis for liver disease has been reported from various sources [1–6]. Research into quantitative analyses for chronic liver disease has been seeing progress, and texture analysis has been the predominant method. Although staging of liver fibrosis has typically been attempted in those studies [1–6], accuracy has not been as high as in liver biopsy. Various studies of quantitative sonographic image analysis for liver tumors have been published [3, 9–11]. These have revealed the
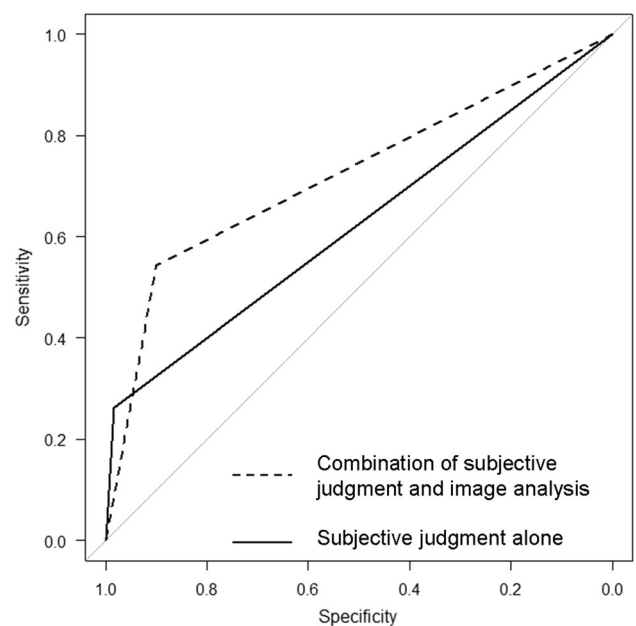

Fig. 5 When either subjective judgment or one image analysis factor was positive, diagnostic accuracy of malignancy was improved over subjective judgment alone

possibility of differentiating between hepatic malignancies and hepatic hemangiomas based on texture analysis using wavelet packets [9], and superior-order co-occurrence matrices [10]. The above investigations aimed at maximizing accuracy for each hepatic nodule using computer-aided algorithms, but morphological features remained unknown. Our results revealed higher circularity and minimum gray values as specific findings compared with HCC and liver metastasis. Imaging analysis can thus provide detailed findings of lesions that human readers may not recognize.

Correlations between subjective judgment and image analysis were good for shape and surface of the hepatic nodules (Fig. 4). Circularity correlated with a round shape, and solidity correlated with a smooth surface. In contrast, no gray values other than standard deviation correlated with subjective judgment of echogenicity. This discrepancy can be explained by the fact that the reviewers judged echogenicity of the hepatic nodules based on differences between the nodule and hepatic parenchyma. On the other hand, the combination of subjective judgment and image analysis improved the diagnostic accuracy for malignancy in this study.

This study has several limitations that need to be considered when interpreting the results. First, free-hand drawing does not provide accurate sampling for the outline of hepatic nodules. Automating the creation of outlines is difficult in this software, even if the image threshold is adjusted. Validation of this free-hand method is provided in Fig. 3. Meanwhile, the minimum gray value does not depend on our measurement procedure, and is considered reliable. Recently, a method for tumor boundary detection using gradient vector flow was reported [17]. This technique would lead to improved quantitativity of image analysis. Second, although this method can be used to analyze two-dimensional images, three-dimensional data cannot be measured. Third, the morphology and color of HCCs and liver metastasis show various forms in each case. For instance, HCCs exhibit several morphological types: early HCC, single nodular type, single nodular type with extra-nodular growth, contiguous multi-nodular type, and poorly demarcated nodular type [18]. Hepatic hemangiomas are affected by patient position and respiration [19].

In the future, this method could be applied to other organs or imaging modalities. We believe that image analysis could "translate" various subjective expressions such as "smooth," "rough," "irregular," or "round" to quantitative data.

References

1. Mailloux GE, Bertrand M, Stampfler R, et al. Texture analysis of ultrasound B-mode images by segmentation. Ultrason Imaging. 1984;6:262–77.
2. Layer G, Zuna I, Loren A, et al. Computerized ultrasound B-scan texture analysis of experimental diffuse parenchymal liver disease: correlation with histopathology and tissue composition. J Clin Ultrasound. 1991;19:193–201.
3. Sujana H, Swarnamani S, Suresh S. Application of artificial neural networks for the classification of liver lesions by image texture parameters. Ultrasound Med Biol. 1996;22:1177–81.
4. Badawi AM, Derbala AS, Youssef AM. Fuzzy logic algorithm for quantitative tissue characterization of diffuse liver diseases from ultrasound images. Int J Med Inform. 1999;55:135–47.
5. Wang Y, Itou K, Taniguchi N, et al. Studies on tissue characterization by texture analysis with cooccurrence matrix method using ultrasonography and CT imaging. J Med Ultrason. 2002;29:211–23.
6. Yamada H, Ebara M, Yamaguchi T, et al. A pilot approach for quantitative assessment of liver fibrosis using ultrasound: preliminary results in 79 cases. J Hepatol. 2006;44:68–75.
7. Jung EM, Clevert DA, Schreyer AG, et al. Evaluation of quantitative contrast harmonic imaging to assess malignancy of liver tumors: a prospective controlled two-center study. World J Gastroenterol. 2007;13:6356–64.
8. Wakui N, Takayama R, Kanekawa T, et al. Usefulness of arrival time parametric imaging in evaluating the degree of liver disease progression in chronic hepatitis C infection. J Ultrasound Med. 2012;31:373–82.
9. Yoshida H, Casalino DD, Keserci B, et al. Wavelet-packet-based texture analysis for differentiation between benign and malignant liver tumours in ultrasound images. Phys Med Biol. 2003;48:3735–53.
10. Mitrea D, Mitrea P, Nedevschi S, et al. Abdominal tumor characterization and recognition using superior-order cooccurrence matrices, based on ultrasound images. Comput Math Methods Med. 2012;2012:348135.
11. Virmani J, Kumar V, Kalra N, et al. Characterization of primary and secondary malignant liver lesions from B-mode ultrasound. J Digit Imaging. 2013;26:1058–70.
12. ImageJ User guide. V Menu commands 30 Analyze. Available from http://imagej.nih.gov/ij/docs/guide/146-30.html#toc-Subsection-30.2.
13. Makuuchi M, Hasegawa H, Yamazaki S, et al. Ultrasonic characteristics of the small hepatocellular carcinoma. Ultrasound Med Biol. 1983;489–91.
14. Mirk P, Rubaltelli L, Bazzocchi M, et al. Ultrasonographic patterns in hepatic hemangiomas. J Clin Ultrasound. 1982;8:373–8.
15. Ito H, Tsujimoto F, Nakajima Y, et al. Sonographic characterization of 271 hepatic hemangiomas with typical appearance on CT imaging. J Med Ultrasonics. 2012;39:61–8.

16. Yoshida T, Matsue H, Okazaki N, et al. Ultrasonographic differentiation of hepatocellular carcinoma from metastatic liver cancer. J Clin Ultrasound. 1987;15:431–7.

17. Le Y, Xianze Xu, Li Zha, et al. Tumor boundary detection in ultrasound imagery using multi-scale generalized gradient vector flow. J Med Ultrasound. 2015;42:25–38.

18. Kanai T, Hirohashi S, Upton MP, et al. Pathology of small hepatocellular carcinoma. A proposal for a new gross classification. Cancer. 1987;60:810–9.

19. Tsujimoto F, Abe T, Murakami Y, et al. Temporal changes of internal echoes in hepatic hemangiomas. J Jpn Radiol Soc. 1989;49:574–82.